Available online at www.sciencedirect.com
SCIENCE DIRECT®
International Journal of Solids and Structures 43 (2006) 346–356
INTERNATIONAL JOURNAL OF SOLIDS and STRUCTURES
www.elsevier.com/locate/ijsolstr

Bending of layers weakened by cuts

L.A. Fil'shtinskii [a], Yu.D. Kovalev [a], E.S. Ventsel [b,*]

[a] *Department of Mathematical Physics, Sumy State University, 40007 Sumy, Ukraine*
[b] *Department of Engineering Science and Mechanics, The Pennsylvania State University, 250A Earth, Engineering Sciences Building, University Park, PA 16802, USA*

Received 31 August 2004; received in revised form 23 May 2005
Available online 20 July 2005

Abstract

In the present paper, a method proposed by one of the authors is extended to a class of skew-symmetric elastic problems for the stress analysis of a layer supported by sliding fixed supports and weakened by several stress raisers. The corresponding boundary value problem is reduced to an infinite system of one-dimensional singular integral equations of the second kind. The expressions for the stress components in an elastic layer weakened by stress raisers are presented. Based on the developed analytical algorithm, extensive numerical investigations have been conducted. The results of these investigations are illustrated graphically exposing some novel qualitative and quantitative knowledge about stress concentration in the layer depending on some geometric parameters of stress raisers and Poisson's ratio of a layer material.
© 2005 Elsevier Ltd. All rights reserved.

Keywords: Elastic layer; Stress concentration; Singular integral equations; Stress raiser

1. Introduction

The stress concentration problem in the modern mechanical engineering is critical because it is associated with durability and reliability of projected machines and structures and their components. Stress raisers in such structures can occur as a result of material composition imperfections (cavities, flaws, foreign inclusions) or they can be caused by technological and structural needs (holes, cuts, etc.). In both cases, analyzing the effect of single and multiple stress raisers, as well as their mutual effect on a stress state of structural components is very important. The accurate analysis of stress states in structures near stress raisers demands a

* Corresponding author. Tel.: +1 814 865 4523; fax: +1 814 863 7967.
E-mail address: ventsel@psu.edu (E.S. Ventsel).

0020-7683/$ - see front matter © 2005 Elsevier Ltd. All rights reserved.
doi:10.1016/j.ijsolstr.2005.06.019

three-dimensional problem statement (Chen et al., 2000; Chung and Pon, 2001; Matysiak and Pauk, 1999; Meshii and Woctanabe, 1998; Noda et al., 1998; Sundara Raja Iyengar et al., 1988; Sih et al., 1966).

The efficient homogeneous solutions method (HSM) was developed by Lur'ye (1942) for solving three-dimensional problems. This method was generally employed by Grigoluk et al. (1995), Kosmodamianskii and Shaldyrvan (1978), Fil'shtinskii et al. (2002), and Sundara Raja Iyengar et al. (1988) for the stress analysis in layers weakened by various stress raisers. Another efficient method, the eigen-vector function method, has been employed by Grinchenko and Ulitko (1970) for solving three-dimensional problems, in particular, the Kirsch problem for a layer. A different approach to solving three-dimensional elastic problems for thick-walled orthotropic cylinders has been proposed by Grigorenko et al. (2001).

The HSM is very efficient in the construction of a set of particular solutions for a layer (cylinder) having any boundary conditions on its bases. If the boundary conditions are of the "crossed type" (sliding fixed ends or layer bases are attached to a diaphragm that is absolutely rigid in its plane and is flexible in out-of-plane direction), then the resulting boundary value problem becomes somewhat simpler. Such problems are said to periodic with respect to one of the coordinates. The procedure for solving such periodic problems of the theory of elasticity and electro elasticity for a piecewise homogeneous cylinder in R^3, different from Lur'ye's method, was proposed by Fil'shtinskii (1990). The problem of stretching and bending of a layer weakened by a through-thickness crack for homogeneous by stresses boundary conditions on the layer bases, has been considered by Fil'shtinskii et al. (2002).

In this paper, a mixed skew-symmetric elasticity problem for a layer weakened by two through-thickness cavities-cuts with mixed boundary conditions on its bases is considered. A distinctive feature of the present investigation lies in the fact that the homogeneous solutions are constructed with the use of the procedure proposed by one of the authors (Fil'shtinskii, 1990). This procedure does not exploit the highly cumbersome symbolic Lur'ye's method. Furthermore, one-dimensional singular integral equations, or more precisely, an infinite system of such equations, are used for solving the three-dimensional boundary value problem for a cylindrical body.

The conducted numerical investigations have shown a rapid convergence of the solution of the system of singular integral equations throughout the entire range of the "thickness" coordinate. Thus, the proposed procedure actually reduces the involved problem dimensionality by two.

2. The problem statement and the method of solution

Let us consider an elastic layer $-h \leqslant x_3 \leqslant h$, $-\infty < x_1, x_2 < \infty$, weakened by two through-thickness cuts-cavities situated along the x_3 axis. The cross sections of these cuts-cavities represent nonintersecting and sufficiently smooth contours L_n $(n = 1, 2)$ $(L_1 | L_2 = \Theta)$. Let a surface load (N, T, Z) be applied on the cut boundaries and no loading is applied on an infinity. We assume that the components of the given loading are expanded into Fourier series in the x_3 coordinate on $[-h, h]$. Let the following conditions hold on the layer ends:

$$u_3(x_1, x_2, \pm h) = \sigma_{13}(x_1, x_2, \pm h) = \sigma_{23}(x_1, x_2, \pm h) = 0. \tag{2.1}$$

The components of the displacement vector can be written in the form:

$$\begin{aligned} u_i &= \sum_{k=0}^{\infty} u_{ik}(x_1, x_2) \sin \gamma_k x_3, \quad (i = 1, 2), \\ u_3 &= \sum_{k=0}^{\infty} u_{3k}(x_1, x_2) \cos \gamma_k x_3, \quad \gamma_k = \frac{2k+1}{2h}\pi. \end{aligned} \tag{2.2}$$

The above representations of the displacement vector components satisfy automatically conditions (2.1) on the ends of the layer.

After separating the variables in the Lame equations, we obtain the following system:

$$\begin{aligned}&\kappa_k u_{ik} + \sigma\partial_i\theta_k = 0, \quad \kappa_k u_{3k} + \sigma\gamma_k\theta_k = 0,\\ &\kappa_k = \Delta - \gamma_k^2, \quad \Delta = \partial_1^2 + \partial_2^2, \quad \theta_k = \partial_1 u_{1k} + \partial_2 u_{2k} - \gamma_k u_{3k},\\ &\partial_i = \partial/\partial x_i \quad (i = 1, 2), \quad \sigma = (1 - 2\nu)^{-1}.\end{aligned} \tag{2.3}$$

Eq. (2.3) can be integrated in the following manner. Taking into account that θ_k is a metaharmonic function,one can introduce an arbitrary solution to the equation $\kappa_k^2\psi_k = 0$. Let us assume that $\theta_k = \kappa_k\psi_k$. This provides a way to obtain the following:

$$\begin{aligned}&u_{1k} = -\sigma\partial_1\Omega_k + \sigma\partial_2\Omega_k^*, \quad u_{2k} = -\sigma\partial_2\Omega_k - \sigma\partial_1\Omega_k^*,\\ &u_{3k} = -\gamma_k\sigma\Omega_k + \Phi_k, \quad k_k\Omega_k^* = 0, \quad k_k\Phi_k = 0 \quad (k = 0, 1, \ldots),\end{aligned} \tag{2.4}$$

where Ω_k^* and Φ_k are arbitrary metaharmonic functions. Then we require that the expressions (2.4) satisfy the equality $\theta_k = \kappa_k\Omega_k$. This leads to the following representations:

$$u_{1k} - \mathrm{i}u_{2k} = 2\sigma\frac{\partial}{\partial z}(\mathrm{i}\Omega_k^* - \Omega_k), \quad u_{3k} = -\left(\frac{1+\sigma}{\gamma_k}\kappa_k + \sigma\gamma_k\right)\Omega_k, \quad \frac{\partial}{\partial z} = \frac{1}{2}(\partial_1 - \mathrm{i}\partial_2), \quad z = x_1 + \mathrm{i}x_2. \tag{2.5}$$

The formulas (2.2) and (2.5) yield the expressions for elastic displacements in the layer in terms of the functions Ω_k^* and Ω_k, where Ω_k^* (vortex solution) describes a rotation of an element about the Ox_3 axis: $\partial_2 u_{1k} - \partial_1 u_{2k} = \sigma\Delta\Omega_k^*$.

The integral representations of the functions θ_k, Ω_k^* and Ω_k are taken in the form:

$$\begin{aligned}&\theta_k(z) = \sum_{j=1}^{2}\int_{L_j} p_{jk}(\zeta_j)K_0(\gamma_k r_j)\,\mathrm{d}s_j + \frac{2}{\gamma_k}\mathrm{Re}\int_{L_j} q_{jk}(\zeta_j)\frac{\partial}{\partial\zeta_j}K_0(\gamma_k r_j)\,\mathrm{d}\zeta_j,\\ &\mathrm{i}\Omega_k^*(z) - \Omega_k(z) = \sum_{j=1}^{2}\frac{2\mathrm{i}}{\gamma_k}\int_{L_j}\bar{q}_{jk}^*(\zeta_j)\frac{\partial}{\partial\bar{\zeta}_j}K_0(\gamma_k r_j)\,\mathrm{d}\bar{\zeta}_j + \frac{1}{\gamma_k^2}\mathrm{Re}\int_{L_j} q_{jk}(\zeta_j)\frac{\partial}{\partial\zeta_j}(r_j K_1(\gamma_k r_j))\,\mathrm{d}\zeta_j,\\ &\qquad r_j = |\zeta_j - z|, \quad \zeta_j = \xi_j + \mathrm{i}\eta_j \in L_j, \quad z = x_1 + \mathrm{i}x_2,\end{aligned} \tag{2.6}$$

where $K_n(\gamma_k r)$ is the Macdonald function of order n, ds is an arc element of contour L; the densities $p_{jk}(\zeta_j)$, $q_{jk}(\zeta_j)$, and $q_{jk}^*(\zeta_j)$ are not yet known.

The boundary conditions on L are written in the complex form as follows:

$$\begin{aligned}&(\sigma_{11} + \sigma_{22}) - \mathrm{e}^{2\mathrm{i}\psi}(\sigma_{22} - \sigma_{11} + 2\mathrm{i}\sigma_{12}) = 2(N - \mathrm{i}T),\\ &\mathrm{Re}[\mathrm{e}^{-\mathrm{i}\psi}(\sigma_{13} + \mathrm{i}\sigma_{23})] = Z,\end{aligned} \tag{2.7}$$

where ψ is an angle between the outward normal to the boundary of the cavity-cut and the Ox_1 axis.

Using Hooke's law and the formulas (2.5), one can represent the conditions (2.7) in the following form:

$$\begin{aligned}&2\sigma\mathrm{e}^{2\mathrm{i}\psi}\left\{\frac{\partial^2}{\partial z^2}(\mathrm{i}\Omega_k^* - \Omega_k)\right\} - \frac{1}{2}\theta_k - \frac{1}{2}\sigma\gamma_k^2\Omega_k = \frac{1}{2\mu}(N_k - \mathrm{i}T_k),\\ &\mathrm{Re}\left\{\mathrm{e}^{\mathrm{i}\psi}\left[\sigma\gamma_k\frac{\partial}{\partial z}(\mathrm{i}\Omega_k^* - \Omega_k) - \frac{\partial}{\partial z}\left(\sigma\gamma_k\Omega_k + \frac{1+\sigma}{\gamma_k}\theta_k\right)\right]\right\} = \frac{1}{2\mu}Z_k.\end{aligned} \tag{2.8}$$

3. The system of singular integral equations

By using the the passage to the limit and the representation (2.6), the boundary value problem (2.8) is reduced to the following system of six singular integral equations (for each fixed value of k)

$$\begin{aligned} &\omega_{n2k}a_k + \omega_{n3k}b_k + \sum_{j=1}^{2}\sum_{i=1}^{3}\int_{L_j}\omega_{jik}G_{jik}^{(n)}\,\mathrm{d}s_j = \frac{1}{2\mu}(N_k^{(n)} - \mathrm{i}T_k^{(n)}),\\ &\omega_{n1k}c_k + \sum_{j=1}^{2}\sum_{i=1}^{3}\int_{L_j}\omega_{jik}G_{jik}^{*(n)}\,\mathrm{d}s_j = \frac{1}{2\mu}Z_k^{(n)}, \end{aligned} \tag{3.1}$$

where

$$a_k = \frac{\pi\mathrm{i}(1+\sigma)}{2\gamma_k},\quad b_k = \frac{\pi(1+\sigma)}{2\gamma_k},\quad c_k = -b_k,$$

$$G_{j1k}^{(n)}(\zeta_j,\zeta_{n0}) = \frac{\sigma\gamma_k}{4}r_{jn0}K_1(\gamma_k r_{jn0})(\mathrm{e}^{2\mathrm{i}(\psi_{n0}-\alpha_{jn0})}+1) - \frac{1}{2}K_0(\gamma_k r_{jn0}),$$

$$\begin{aligned} G_{j2k}^{(n)}(\zeta_j,\zeta_{n0}) = {}& \frac{\sigma\gamma_k}{4}r_{jn0}K_0(\gamma_k r_{jn0})\left[\sin(\psi_j-\alpha_{jn0}) - \frac{\mathrm{i}\mathrm{e}^{2\mathrm{i}\psi_{n0}}}{2}h_{1j}^{(n)}(\psi_j,\alpha_{n0})\right]\\ &+K_1(\gamma_k r_{jn0})\left\{\frac{\sigma}{2}\sin(\psi_j-\alpha_{jn0}) + \frac{\mathrm{i}\mathrm{e}^{2\mathrm{i}\psi_{n0}}}{2}\left[(1+\sigma)\mathrm{e}^{-\mathrm{i}(\psi_j+\alpha_{jn0})} - \frac{\sigma}{2}h_{2j}^{(n)}(\psi_j,\alpha_{in_0})\right]\right\}, \end{aligned}$$

$$\begin{aligned} G_{2k} = (\xi,\xi_0) = {}& \frac{z\gamma_k}{4}rK_0(\gamma_k r)\left[\sin(\psi-\alpha_0) - \frac{\mathrm{i}\mathrm{e}^{2\mathrm{i}\psi_0}}{2}h_1(\psi,\alpha_0)\right]\\ &+K_1(\gamma_k r)\left\{\frac{\sigma}{2}\sin(\psi-\alpha_0) + \frac{\mathrm{i}\mathrm{e}^{2i\psi_0}}{2}\left[(1+\sigma)\mathrm{e}^{-\mathrm{i}(\psi+\alpha_0)} - \frac{\sigma}{2}h^2(\psi,\alpha_0)\right]\right\}, \end{aligned}$$

$$h_{1j}^{(n)}(\psi_j,\alpha_{jn0}) = \mathrm{e}^{\mathrm{i}(\psi_j-3\alpha_{jn0})} - \mathrm{e}^{-\mathrm{i}(\psi_j+\alpha_{jn0})},$$

$$h_{2j}^{(n)}(\psi_j,\alpha_{jn0}) = \mathrm{e}^{\mathrm{i}(\psi_j-3\alpha_{jn0})} - \mathrm{e}^{-\mathrm{i}(\psi_j+\alpha_{jn0})},$$

$$G_{j1k}^{*(n)}(\zeta_j,\zeta_{n0}) = \frac{1}{2}[\sigma\gamma_k r_{jn0}K_0(\gamma_k r_{jn0}) - (1+\sigma)K_1(\gamma_k r_{jn0})]\cos(\psi_{n0}-\alpha_{jn0}),$$

$$\begin{aligned} G_{j2k}^{*(n)}(\zeta_j,\zeta_{n0}) = {}& \frac{\sigma\gamma_k}{4}r_{jn0}K_1(\gamma_k r_{jn0})[\sin(\psi_{n0}+\psi_j-2\alpha_{jn0}) - \sin(\psi_{n0}-\psi_j)]\\ &-\frac{1}{2}K_0(\gamma_k r_{jn0})\sin(\psi_{n0}-\psi_j), \end{aligned}$$

$$\begin{aligned} G_{j3k}^{*(n)}(\zeta_j,\zeta_{n0}) = {}& \frac{\sigma\gamma_k}{4}r_{jn0}K_1(\gamma_k r_{jn0})[\cos(\psi_{n0}+\psi_j-2\alpha_{jn0}) + \cos(\psi_{n0}-\psi_j)]\\ &+\frac{1}{2}K_0(\gamma_k r_{jn0})\cos(\psi_{n0}-\psi_j), \end{aligned}$$

$$q_{jk}^{*} = \frac{\mathrm{i}(1+\alpha)}{\sigma\gamma_k^2}q_{jk},$$

$$\omega_{j1k} = p_{jk},\quad \omega_{j2k} = \mathrm{Re}\,q_{jk},\quad \omega_{j3k} = \mathrm{Im}\,q_{jk},$$

$$\zeta_j - \zeta_{n0} = r_{jn0}\mathrm{e}^{\mathrm{i}\alpha_{jn0}},\quad \zeta_{n0} = \xi_{n0} + \mathrm{i}\eta_{n0} \in L_n.$$

Here ω_{jik} are unknown densities to be determined.

4. The numerical results and discussion

As an example,we consider a layer weakened by two through-thickness cuts having either elliptic cross section

$$L_1: \xi_{11} = R_{11}\cos\varphi_1 + d_{11}, \quad \xi_{21} = R_{21}\sin\varphi_1 + d_{21}, \quad 0 \leqslant \varphi_1 \leqslant 2\pi,$$
$$L_2: \xi_{12} = R_{12}\cos\varphi_2 + d_{12}, \quad \xi_{22} = R_{22}\sin\varphi_2 + d_{22}, \quad 0 \leqslant \varphi_2 \leqslant 2\pi$$

or square cross section (squares with rounded off corners)

$$L_1: \xi_{11} = a(\cos\varphi_1 + c\cos 3\varphi_1) + d_{11},$$
$$\xi_{21} = (a\sin\varphi_1 - c\sin 3\varphi_1) + d_{21}, \quad 0 \leqslant \varphi_1 \leqslant 2\pi,$$
$$L_2: \xi_{12} = a(\cos\varphi_2 + c\cos 3\varphi_2) + d_{12},$$
$$\xi_{22} = a(\sin\varphi_2 - c\sin 3\varphi_2) + d_{22}, \quad 0 \leqslant \varphi_2 \leqslant 2\pi, \ c = 0,14036,$$

The layer is subjected to load $N = Px_3$ ($P = \text{const.}$) applied on the cut surfaces.

In the numerical implementation of the algorithm,the system of integral equations was reduced to the system of linear algebraic equations by the mechanical quadrature method developed by Erdogan et al. (1973).

To characterize the state of stress on the surface of the cut,the following stress was calculated:

$$\sigma_{\theta\theta} = \sigma_{11}\sin^2\theta + \sigma_{22}\cos^2\theta - 2\sigma_{12}\cos\theta\sin\theta,$$
$$\theta = \psi - \pi. \tag{4.1}$$

The numerical procedure of the developed method involves the following steps: at first, the system of the integral equations was solved, then the Fourier coefficients of the stress tensor, $\sigma_{ij}^{(k)}$, were determined, and thereafter-unknown stresses on the surfaces of the corresponding cut were calculated.

The diagrams of the distribution of the relative circumferential stress $\sigma_1 = -\sigma_{\theta\theta}/P$ are shown in Figs. 1–10:

(i) along the "thickness" coordinate at the point where the above stress takes on the maximum value (Figs. 1, 3, 5 and 8);
(ii) along the contour of the generator of the cylindrical surface (Figs. 2, 4, 6, 7, 9 and 10).

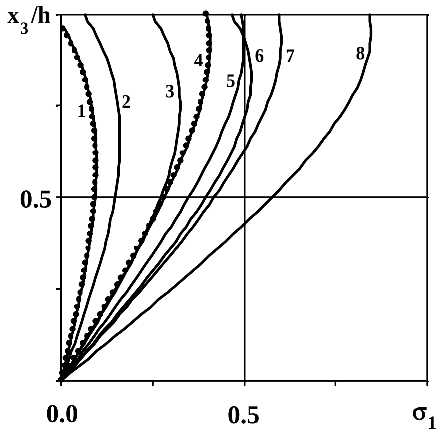

Fig. 1. Distribution of the relative circumferential stress over the layer thickness for circular cuts.

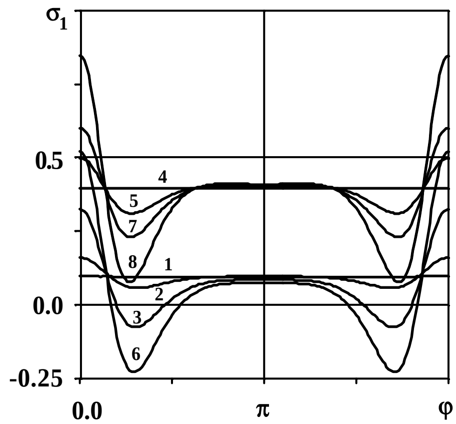

Fig. 2. Distribution of the relative circumferential stress along the generator of the cylindrical surface for circular cuts.

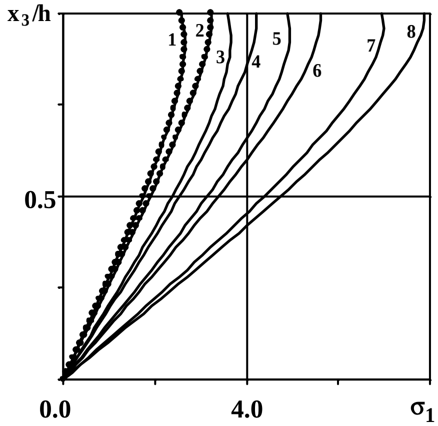

Fig. 3. Distribution of the relative circumferential stress over the layer thickness for circular cuts.

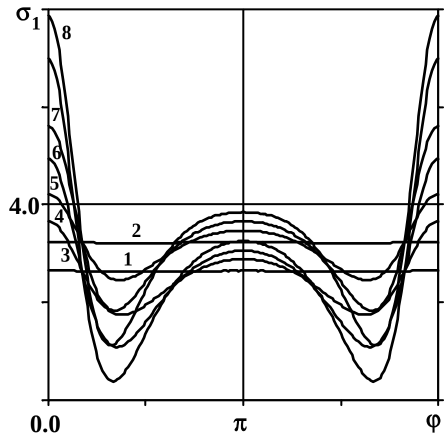

Fig. 4. Distribution of the relative circumferential stress along the generator of the cylindrical surface for circular cuts.

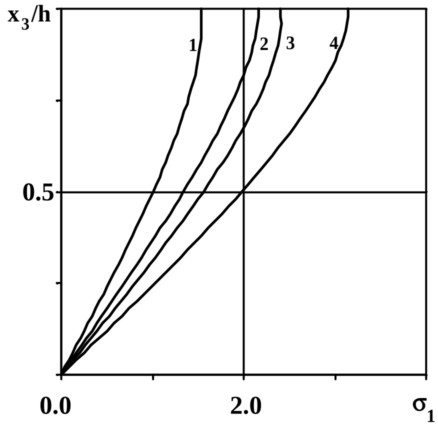

Fig. 5. Distribution of the relative circumferential stress over the layer thickness for cuts having the square cross section.

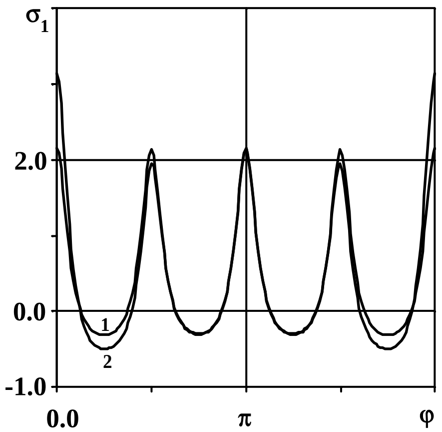

Fig. 6. Distribution of the relative circumferential stress along the generator of the cylindrical surface for cuts having the square cross section.

Numerical results were obtained for various Poisson's ratios ν. In what follows, the results obtained by the proposed method are said to be approximate while the results of the axisymmetric problem of the theory of elasticity by the series method are exact.

Let for the sake of definiteness, the contours L_2 and L_1 are arranged to the left and to the right of the $0x_2$, respectively. Let the cut centers are located on the $0x_1$ axis. In this case, denote the distance between the above centers as l_x. Thus

$$l_x = |d_{11}| + |d_{12}|, \quad (d_{21} = d_{22} = 0).$$

The data given in Figs. 1–4 refer to the contour L_2 for the case of circular cuts of the following geometry

$$R_{11} = R_{21} = R_{12} = R_{22} = R = 1 \quad (\varphi_1 = \varphi_2 = \varphi).$$

The curves 1–3, and 6 were constructed at the point $\varphi = 0$ for the following data: $h/R = 1$; $l_x/R = 8$, 4, 3, and 2.5, respectively, The curves 4, 5, 7, and 8 in Fig. 1 were constructed at point $\varphi = 0$ for the following

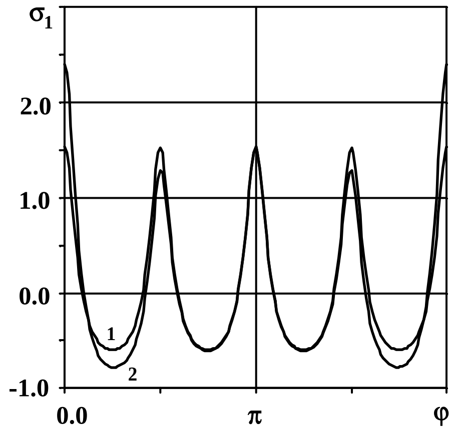

Fig. 7. Distribution of the relative circumferential stress along the generator of the cylindrical surface for cuts having the square cross section.

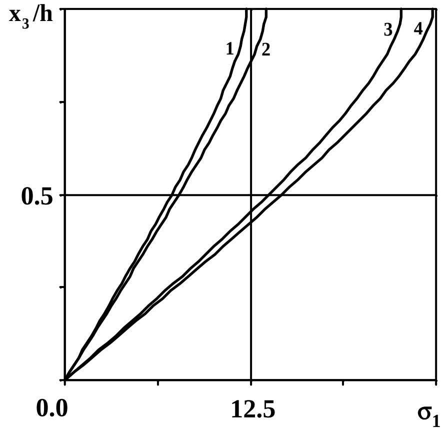

Fig. 8. Distribution of the relative circumferential stress over the layer thickness for cuts having the square cross section.

data: $h/R = 1$; $l_x/R = 6$, 3.5, 3, and 2.5, respectively, $\upsilon = 0.15$. The curves 1 and 4 refer to the layer having just one stress raiser. The points on the curves 1 and 4 correspond to the exact solution of axisymmetric problem of the theory of elasticity for the layer weakened by one through-thickness cut. It should be noted a good agreement between the exact and approximate solutions.

Fig. 2 shows the distribution of the circumferential stresses σ_1 along the generator of the cylindrical surface at various sections over the thickness of the layer where the above stresses take on the maximum values. The curves 1–8 in Fig. 2 are found to fit the mechanical and geometrical parameters with the analogous curves in Fig. 1. The curves 1 and 4 were given for the values of the "thickness" coordinates $x_3 = 0.6h$ and $x_3 = 0.92h$, respectively. The curves 1 and 4 degenerate into straight lines. This corresponds to the lack of mutual impact of the two stress raisers. The values of the stresses given on these curves,agree well with the corresponding solutions to axisymmetric problems of the theory of elasticity for the layer weakened by just one circular cut. The curves 2, 3, 5–8 are given at sections $x_3 = 0.66h$, $0.76h$, $0.92h$, $0.82h$, $0.94h$, and $0.94h$, respectively.

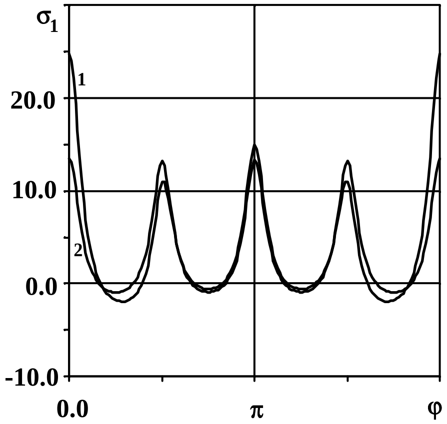

Fig. 9. Distribution of the relative circumferential stress along the generator of the cylindrical surface for cuts having the square cross section.

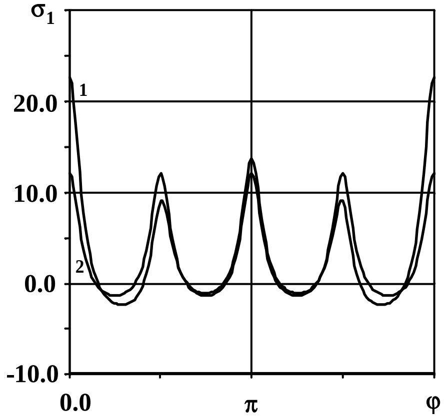

Fig. 10. Distribution of the relative circumferential stress along the generator of the cylindrical surface for cuts having the square cross section.

The curves 1, 3, 5, and 7 in Fig. 3 were constructed at the point $\varphi = 0.$ for the following data: $h/R = 4$, $l_x/R = 16, 4, 3$, and 2.5, respectively; $\upsilon = 0.4$. The curves 2, 4, 6, and 8 in Fig. 3 were constructed at the point $\varphi = 0$ for the following data: $h/R = 4$; $l_x/R = 14, 4, 3$, and 2.5, respectively; $\upsilon = 0.15$. The curves 1 and 2 refer to the layer with one stress raiser. The points on the curves 1 and 2 refer to the results of the exact solution to the corresponding axisymmetric problem of the theory of elasticity for the layer weakened by one cut. Here it is also seen that the results of the approximate and exact solutions are in a good agreement.

Fig. 4 shows the distribution of σ_1 along the contour of the generator of the cylindrical surface of various sections over the layer thickness. The curves 1–8 in Fig. 4 are found to fit mechanical and geometrical parameters with the analogous curves in Fig. 3. The curves 1–8 were constructed at sections $x_3 = 0.92h$, $0.98h$, $0.94h$, $0.98h$, $0.94h$, $0.98h$, $0.96h$, and $0.98h$, respectively. The curves 1 and 2 correspond to the case when the effect of the mutual impact of the two stress raisers in the layer becomes insignificant. The values given on the above curves agree well with the corresponding solutions to axisymmetric problem of the theory of elasticity for the layer weakened by just one circular cut.

The curves shown in Figs. 5–10 correspond to the contour L_2 in the case of the cuts having the square cross section $\varphi_1 = \varphi_2 = \varphi(0 \leqslant \varphi \leqslant 2\pi)$. The curves 1 and 3 in Fig. 5 were constructed at the point $\varphi = 0$ for the following data: $h/a = 1$; $l_x/a = 6$ and 2.5, respectively; $\upsilon = 0.4$. The curves 2 and 4 were constructed at the point $\varphi = 0$ for the following data: $h/a = 1$; $l_x/a = 5$ and 2.5, respectively; $\upsilon = 0.15$. The curves 1 and 2 refer to the layer with one stress raiser.

Figs. 6 and 7 show the distribution of the stress σ_1 along the contour of the generator of the cylindrical surface at various sections over the layer thickness. The curves 1 and 2 in Fig. 6 are found to fit the mechanical and geometrical parameters with the curves 2 and 4 in Fig. 5, respectively, while the curves 1 and 2 in Fig. 7 with the curves 1 and 3 in Fig. 5, respectively. The curves 1 and 2 in Fig. 6 were constructed at section $x_3 = 0.98h$ while the curves 1 and 2 in Fig. 7—at section $x_3 = 0.96h$.

The curves 1 and 3 in Fig. 8 were constructed at the point $\varphi = 0$ for the following data: $h/a = 4$; $l_x/a = 12$ and 2.5, respectively; $\upsilon = 0.4$. The curves 2 and 4 in Fig. 8 were constructed at the point $\varphi = 0$ for the following data: $h/a = 4$; $l_x/a = 8$ and 2.5, respectively; $\upsilon = 0.15$. The curves 1 and 2 in this figure refer to the case of the presence of just one stress raiser in the layer.

Figs. 9 and 10 show the distribution of the stress σ_1 along the contour of the generator of the cylindrical surface at various sections over the layer thickness. The curves 1 and 2 are found to fit the mechanical and geometrical parameters with the curves 4 and 2, respectively, in Fig. 8 while the curves 1 and 2 in Fig. 10 with the curves 3 and 1 in Fig. 8, respectively. The curves 1 and 2 in Figs. 9 and 10 were constructed at section $x_3 = 0.98h$.

5. Conclusion

The following conclusions can be made from the conducted numerical investigation:

(i) A growth of the relative circumferential stress occurs as the intercentral distance or Poisson's ratio decrease;
(ii) As Poisson's ratio increases the maximum value of the relative circumferential stress is displaced from the layer base to its depth;
(iii) The presence of the second cut in the layer becomes insignificant for:

$l_x/R = 6$ when $h/R = 1$ and $\upsilon = 0.15$,
$l_x/R = 8$ when $h/R = 1$ and $\upsilon = 0.4$,
$l_x/R = 14$ when $h/R = 4$ and $\upsilon = 0.15$,
$l_x/R = 16$ when $h/R = 4$ and $\upsilon = 0.4$,
$l_x/a = 5$ when $h/a = 1$ and $\upsilon = 0.15$,
$l_x/a = 6$ when $h/a = 1$ and $\upsilon = 0.4$,
$l_x/a = 8$ when $h/a = 4$ and $\upsilon = 0.15$,
$l_x/a = 12$ when $h/a = 4$ and $\upsilon = 0.4$.

Thus a growth of the effective area of the mutual impact of the two stress raisers is closely associated with the increase in Poisson's ratio and layer thickness.

References

Chen, R., Xue, S., Chen, Z., Chen, J., 2000. The numerical solutions of Green's functions for transversally isotropic elastic strata. Appl. Math. Mech. 21, 49–58.

Chung, Y.-L., Pon, C.-F., 2001. Boundary element analysis of cracked film-substrate media. Int. J. Solids Struct. 38, 75–90.

Erdogan, G.D., Gupta, T.S., Cook, T.S., 1973. The numerical solutions of singular integral equations. In: Method of Analysis and Solutions of Crack Problems. Noordhoff International Publishing, Leyden, pp. 268–425.

Fil'shtinskii, L.A., Kovalev, Yu.D., Ventsel, E.S., 2002. Solution of the elastic boundary problems for a layer with tunnel stress raisers. Int. J. Solids Struct. 39, 6385–6402.

Fil'shtinskii, L.A., 1990. Periodical solutions of some elastic and electrostatic problems for a cylinder in R^3. Theoret. Appl. Mech. 21, 13–20 (in Russian).

Grigoluk, E.I., Kovalev, Yu.D., Fil'shtinskii, L.A., 1995. The bending of a semi-layer weakened by through-thickness opening. Rep. Russ. Acad. Sci. 345, 54–56 (in Russian).

Grigorenko, Y.M., Krukov, N.N., Krizhanovskaya, T.V., 2001. An investigation of stress state of ortotropic hollow cylinders in unsymmetrical loading. Theoret. Appl. Mech. 33, 3–6 (in Russian).

Grinchenko, V.T., Ulitko, A.F., 1970. An exact solution of the Kirsch problem. Prikl. Mekh. Matem. 6, 10–17 (in Russian).

Kosmodamianskii, A.S., Shaldyrvan, V.A., 1978. Thick multiply connected plates. Nauk. Dumk, Kiev (in Russian).

Lur'ye, A.I., 1942. To the theory of thick plates. Prikl. Mekh. Matem. 6, 151–168 (in Russian).

Matysiak, S.J., Pauk, V.J., 1999. On crack problems in an elastic ponderable layer. Int. J. Fract. 96 (4), 371–380.

Meshii, T., Woctanabe, K., 1998. Simplified equations to evaluate the stress intensity factor of an arbitrarily located circumferential crack in a finite cylinder under axisymmetric bending. Nikon Kikai Gakkai Ronbunshu, A (Trans. Jpn. Soc. Mech. Eng. A) 625, 2361–2366.

Noda, N.-A., Tomari, H., Matsuo, T., 1998. Interaction effect between ellipsoidal inclusions in an infinite body under asymmetric uniaxial tension. Nikon Kikai Gakkai Ronbunshu, A (Trans. Jpn. Soc. Mech. Eng. A) 622, 1577–1582.

Sih, G.C., Williams, M.L., Swedlow, J.L., 1966. Three dimensional stress distribution near a sharp crack in a plate of finite thickness, AFML, Wright-Patterson Air Force Base, AFML-TR-66-242.

Sundara Raja Iyengar, K.T., Murthy, M.V.V., Bapu Rao, M.N., 1988. Three dimensional elastic analysis of cracked thick plates under bending felds. Int. J. Solids Struct. 24, 683–703.